Nano/micro silver powders for electronic materials

S. GAVRILIU[a]*, M. LUNGU[a], F. GRIGORE[a], D. DONESCU[b], M. GHIUREA[b]

[a]National Institute for Research and Development in Electrical Engineering INCDIE ICPE-CA
Splaiul Unirii no. 313, 030138 Bucharest - 3, Romania
[b]National Research & Development Institute for Chemistry and Petrochemistry - ICECHIM
Splaiul Independentei no. 202, 060021 Bucharest, Romania

The paper presents a new type of structural materials, namely silver nanoparticles deposited on the silver microcrystalline particles, designed to obtain some conductive inks or pastes. It is known that beside optical, thermo-catalytic, photo-catalytic and bactericidal properties, the silver nanoparticles have a low melting temperature and some exceptional sintering characteristics against the bulk material. The sintering of these silver nanoparticles begins at 150 °C, while this process starts in the range of 650…700 °C even for very fine microcrystalline powders. We developed a chemical method for obtaining silver powders with lowered melting point and improved sinterability. The powders were characterized by chemical, UV-VIS, DLS, SEM and TEM analyses.

1. Introduction

The silver particles as flakes, single or in mixtures with spherical or polyhedral particles are used in a broad variety of applications, particularly in the electronics industry for producing conductive adhesives, conductive polymers, thick films, shielding materials, printing inks and pastes. As a result, the production of silver flakes and powders has developed into an industry of its own [1 - 10].

When heat and electrical conduction of flake-form silver powder is compared to that of spherical form ones, a considerable difference in properties was found. The spherical shaped powders have a few contact points between them. The flake-form silver powders realize a lot of cumulated contact points between the flakes surfaces by a layer upon layer package, and as a result phonons and electrons relatively easily transit such surface contacts through, so that the thermal resistance and the electrical resistance are greatly reduced. The silver flakes thus provided superior thermal and electrical conductivity [11].

Silver flakes are generally produced by mechanically milling of silver powders obtained by various techniques, such as chemical precipitation, electrolytic deposition, melt atomizing and salt or oxide decomposition.

The mechanical milling usually requires an organic lubricant, surfactant, or other organic material in order to prevent co-welding between the particles and thereby to inhibit their agglomeration. Also, the lubricants on the surface of silver flakes lead to some improvements in rheology and electrical conductivity [8].

The novelty of our works consists in obtaining of a new type of silver powders consisting of silver nanoparticles (SNPs) deposited on silver microcrystalline particles (SMPs) flakes (F-SMPs) by an efficient and ecological method. These are designed for obtaining of high quality conductive inks and pastes for different coatings in electronics and electrical engineering.

Recent studies shown that beside particular optical, thermo-catalytic, photo-catalytic or antimicrobial properties, the SNPs present some exceptional sintering characteristics such as liquid phase forming as a result of their low melting temperature, in comparison with the bulk material [7, 8]. The sintering of the SNPs begins at 110…150 °C, while this process at fine microcrystalline powders starts in the range of temperature of 650…700 °C. The forming of the melted bridges at low temperatures leads to increasing of the conductive contact point numbers among the silver flakes. It is a great advantage in the manufacturing of some lead free conductive inks and pastes. In this respect, the conductive layers of silver can be obtained by deposition of some SNPs/SMPs dispersed in vehicles suitable for the intended area of applications. For example, pine oil based vehicles are frequently utilized for screen printing applications [12]. The conductive coatings may be deposited on different substrates by various approaches such as spraying, brushing, dipping, roller coating, screen printing, and so on, followed by a suitable annealing at relatively low temperatures.

2. Experimental

The silver powders were achieved in three main steps. In the first step, the SMPs were obtained by an electrochemical method in a cell with a rotating cathode of stainless steel and a sacrificial anode consisting of turnings of pure silver. The deposition process was carried out in d.c. at U = 30 V and I = 90 A, in an $AgNO_3$ solution having a concentration of 3.5 % wt. and pH of 2.5.

The second step consisted in the SMPs milling to obtain F-SMPs with suitable morphology. The F-SMPs were obtained in the high speed planetary ball mill, by wet

milling of the SMPs with 0.3 wt. % oleic acid using steel balls of $\phi 5$ mm, at 400 rpm, for 8 hours. The F-SMPs were then washed and dried in vacuum. The third step involved the SNPs chemical synthesis and their deposition "in situ" on the F-SMPs using the reduction method of Ag^+ ions from an $AgNO_3$ aqueous solution containing the F-SMPs by a tri-sodium citrate solution and a sodium borohydride solution in a $C_6H_5Na_3O_7 \cdot 2H_2O:AgNO_3$ molar ratio of 2:1 and a $NaBH_4:AgNO_3$ molar ratio of 1:1. The tri-sodium citrate is both a reductive agent and an electrostatic stabilizer for SNPs. Also, a PVP solution of 4 wt. % concentration, as a steric stabilizer was used. The tri-sodium citrate and the PVP solutions were dropped in the $AgNO_3$–F–SMPs aqueous suspension heated at 80 °C and vigorously stirred. Then, in the suspension that was rapidly cooled at 4 °C in a bath of water with ice, the $NaBH_4$ solution was dropped, too. The obtained slime was centrifuged at 6000 rpm, for 30 minutes, washed and dried in vacuum. The silver powders were characterized from chemical composition, grain shape and sizes, dimensional distribution of the grains, reflectance and absorbance point of view. In this respect, some chemical, X-ray, UV-VIS, DLS, TEM, SEM and optical microscopy analyses were used. We performed an extraction with toluene for the characterization by UV-VIS absorbance spectrum and DLS analyses of the SNPs deposited on the F-SMPs.

The presented method can be applied for any SNPs/SMPs composition, but by previously studies we established that the proper content of the SNPs in the final SNPs/F-SMPs ranges between 2…40 wt. %.

3. Results and discussion

In this paper are presented the results obtained in the case of the SNPs/SMPs powders having a SNPs content of 30 wt. %.

Fig. 1 and Fig. 2 show the SEM images (ensemble and detail) of the F-SMPs and SNPs/F-SMPs, respectively. These powders consist of coarse particles in form of flakes with a smooth surface, which are suitable for use in conductive adhesives and general purpose inks.
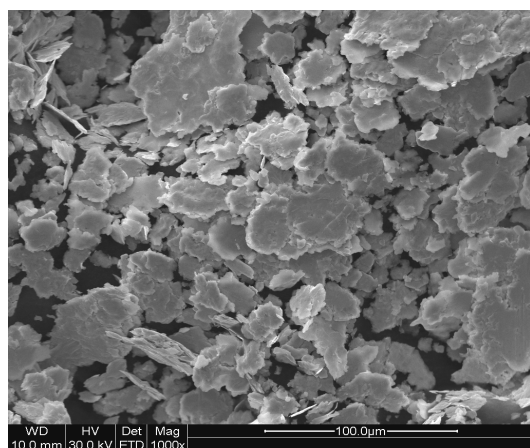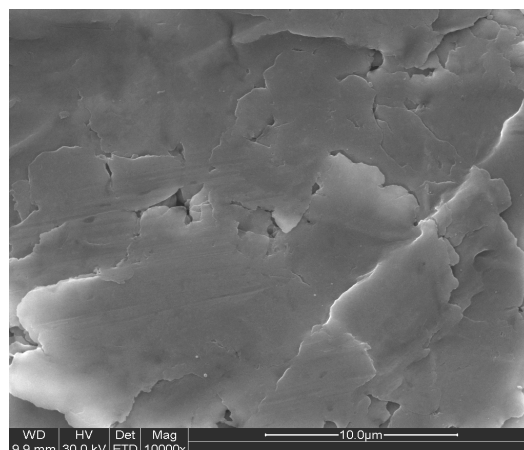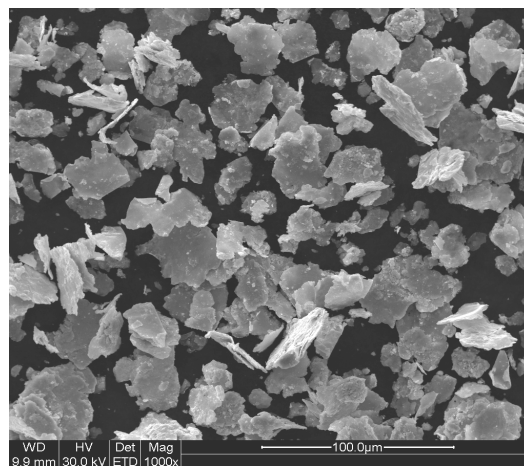

b)

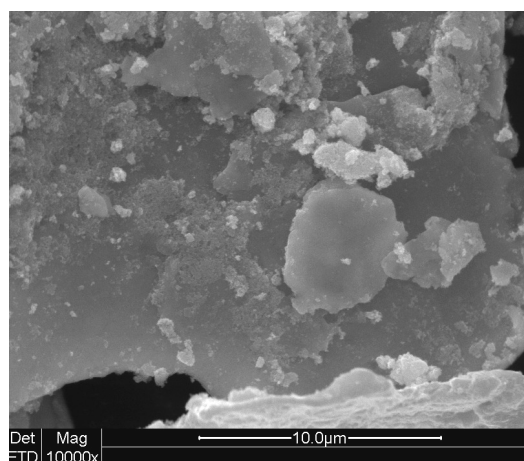Fig. 1. The SEM image of the F-SMPs:
a) ensemble, b) detail.

a)

Fig. 2. The SEM image of the SNPs/F-SMPs:
a) ensemble, b) detail.

a)

The images from Fig. 2 show the deposition of the SNPs on the F-SMPs. The SNPs are uniform dispersed on the F-SMPs surfaces. However, from the facile release of the SNPs from SNPs/F-SMPs observed at the extraction with toluene it seems that the bonding was weak.

Table 1 presents the mean grain sizes of the silver powders. The data from this table prove that the characteristics of the obtained F-SMPs are in agreement to the data presented by the top manufactures in this field, i.e. *Alfa Aesar* silver flakes FS30 having a maximal diameter of 39.2 μm and a tap density of 2.1 g/cm^3 [13].

Table 1. The grain characteristics of the silver powders.

Type of powder	Apparent density, [g/cm^3]	Tap density, [g/cm^3]	d$_{mean}$, [nm]		d$_{max.}$, [μm]
			d$_{FSSS}$ [*]	d$_{XRD}$ [**]	
SMPs	1.43	3.4	3500	116.8	32
F-SMPs	1.33	2.7	1100	30.2	32
SNPs/F-SMPs	1.05	2.7	1170	28.7	32

* d$_{FSSS}$ - Fisher sub-sieve size diameter
** d$_{XRD}$ - average crystallite size calculated from XRD measurements.

The chemical analyses of the all powders type showed a high purity. The impurities content is smaller than 0.02 %.

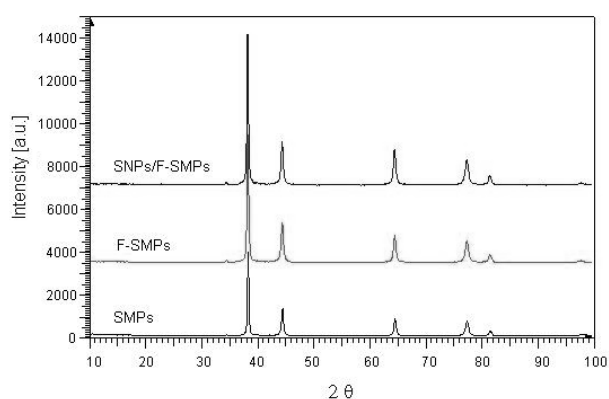Fig. 3 shows the X-ray diffraction patterns of the SMPs, F-SMPs and SNPs/F-SMPs.

Fig. 3. The X-ray diffraction patterns of the SMPs, F-SMPs and SNPs/F-SMPs.

By evaluation of the X-ray patterns resulted that the all types of powders are well crystallized and show typical silver peaks of (111), (200), (220) and (311) corresponding to FCC structure. The (111) planes are the basal facets of the powders. The elementary cell parameters remained unchanged and all presented phases consist in silver micro- and nano-crystallites.

Fig. 4 presents the UV-VIS absorbance spectrum of solution of extracted SNPs from SNPs/F-SMPs powders. The specific yellow color and absorbance peak at the wavelength of 437 nm proved the formation of the SNPs.

It is known that optical spectra of precious metal nanoparticles are dominated by plasmon-polaritons, i.e. collective oscillations of the conduction electrons [14]. The stimulation of these excitations with light leads to pronounced resonances in the optical spectra. The position of the absorbance peaks can vary over a wide spectral range, depending on the preparing particles of different sizes and shapes and by supporting or embedding them on different substrates or in different matrices. Moreover, surface plasmon excitation is accompanied by a drastic increase of the optical near-field in the vicinity of the nanoparticles and this effect is well known as local field enhancement. The position and amplitude of the surface plasmon resonance depend upon the surrounding matrix or supporting substrate material of the nanoparticles. The environment changing of the nanoparticles leads to altering of the dielectric constant and as a result to a red shift of the surface plasmon resonances. A static charge transfer between nanoparticles and supports may take place, which modifies the electron density in the particles and the position of the surface plasmon resonance, which shifts to low energies with decreasing electron concentration. The substrates alters the spill-out of the electrons at the nanoparticles surface, which also causes the shift of the resonance, as can be seen in the reflectance spectrum of SNPs/F-SMPs powders at the wavelength of 466 nm from Fig. 5, comparatively with SNPs solution absorbance at wavelength of 437 nm from Fig. 4.
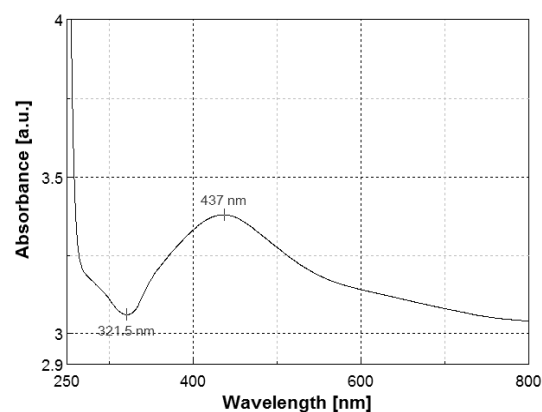

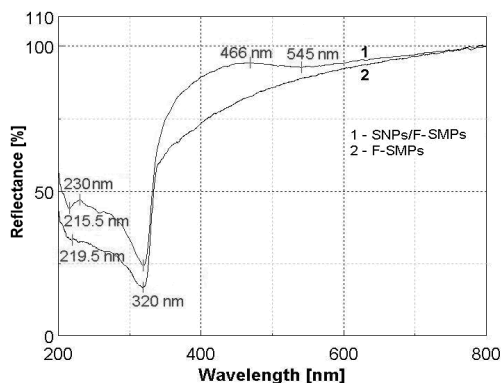*Fig. 4. The absorbance spectrum of the extracted SNPs from SNPs/F-SMPs.*

*Fig. 5. The reflectance spectra of the
F-SMPs and SNPs/F-SMPs.*

Also, in Fig. 5 it is observed that there is a pronounced difference between the reflectance spectrum of the F-SMPs and SNPs/F-SMPs due to the presence of the SNPs, proving the different behavior of the SNPs against the bulk material.

Fig. 6 and Fig. 7, respectively, present the TEM pattern and grain size distribution of the extracted SNPs from SNPs/F-SMPs.
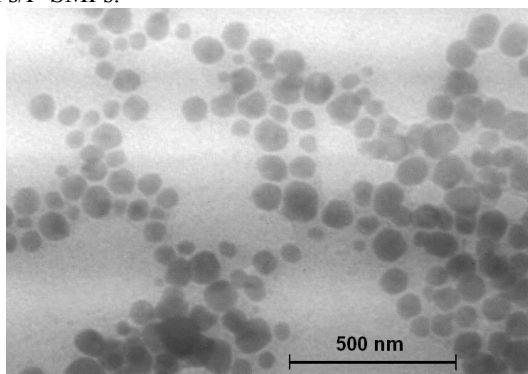

*Fig. 6. The TEM pattern of the extracted
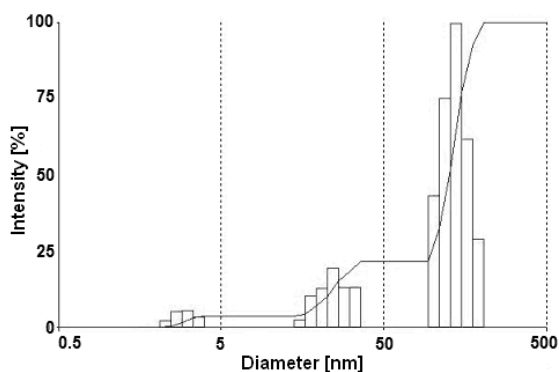SNPs from SNPs/F-SMPs.*

*Fig. 7. The grain size distribution of the extracted
SNPs from SNPs/F-SMPs.*

The TEM pattern (Fig. 6) and the grain size distribution (Fig. 7) of the extracted SNPs from SNPs/F-SMPs show a broad range of the grain size distribution of the SNPs. The mean diameter of the extracted SNPs from SNPs/F-SMPs is 88.9 nm. These results are in accordance with the results

obtained by UV-VIS analyses, too.

4. Conclusions

Based on the presented method, SNPs/SMPs powders having a high purity can be obtained for any composition. The proper content of the SNPs in the final SNPs/F-SMPs ranges between 2…40 wt. %.

The SEM images of the F-SMPs shown that the flake desired morphology was achieved.

The extracted SNPs from SNPs/F-SMPs present an absorbance peak at a wavelength of 437 nm, which is in accordance with the DLS and TEM analyses.

The grain size of the SNPs varies in a broad range.

The SNPs content and their mean diameter are suitable for obtaining of some products with lower melting point against the common F-SMPs.

The presented method is a high-performance one comparatively with the conventional methods for silver powders and flakes producing.

References

[1] J. S. Wang, Patent Appl. Pub. US 2005/0016328 A1, (2005).
[2] E. Khasin, A. Greenboim, US Patent No. 6,012,658, (2000).
[3] M. J. Hampden - Smith, T. T. Kodas, Q. H. Powel, D. J. Skamser, J. Caruso, C. D. Chandler, US Patent No. 6,277,169 B1, (2001).
[4] J. Oprowsky, D. Stotka, US Patent No. 5, 346, 651, (1994).
[5] H. Zosis, Ye. P. Mamunya, L. Apekis, Proc. of the 3rd Int. Conf. on Broad Dielectric Spectroscopy and its Applications, BDS 2004, 23-26 Delft Univ. of Technology, The Nederlands, p. 178, August (2004).
[6] J. Oprowsky, D. Stotka, US Patent No. 5,417,745 (1995).
[7] M. J. Hampden-Smith, T. T. Kodas, Q. H. Powel, D. J. Skamser, J. Caruso, C. D. Chandler, US Patent No.7,004,994 B2 (2006).
[8] J. Rockenberger, F. Zurcher, S. Haubrich, N. Sleiman, US Patent No. 6,878,184, (2005).
[9] T. Sasaki, M. Kato, T. Fujimoto, T. Sakaue, K. Yoshimaro, Patent Appl. Pub. US 2005/0183543 A1, (2005).
[10] U. Bakman, J. K. Jokiniemi, A. Auvinen, K. E. Lehtinen, Journal of Nanoparticle Research, **4,** 325 (2002).
[11] S. H. Park, D. S. Seo, J. K. Lee, Solid State Phenomena Vols. **124 – 126**, 639 (2007).
[12] Jr. Mc Gowan, US Patent No. 4,369,063, (1983).
[13] http://www.azom.com/details.asp? ArticleID=3583#_Silver_Flakes_Product
[14] C. Hendrich, J. Bosbach, F. Stietz, F. Hubenthal, T. Vartanyan, F. Trager, Appl. Phys. **B 76**, 869 (2003).

_____
*Corresponding author: stefgav@icpe-ca.ro